Archives of Mining Sciences **46**, 1 (2001) 85–99

JAN KIEŁBASA*, **

ANGLE-DEPENDENT CHARACTERISTICS OF THERMAL DETECTOR OF FLOW REVERSAL

CHARAKTERYSTYKI KĄTOWE CIEPLNEGO INDYKATORA ZWROTU PRZEPŁYWU

The paper deals with the theoretical and experimentally obtained angle-dependent characteristics of two-wire thermal sensor operating in a bridgeless CTA circuit. The distinctive feature of theoretical curves is that the distance between the wires is provided. A simple case, when the sensor is used as the flow reversal detector, was investigated in the work of Kiełbasa (Kiełbasa 2000a).

Several sensors were tested in a wind tunnel. The detailed procedure was presented in the quoted paper. The sensor, fitted in a rotating holder, was placed in the wind tunnel. The measured parameter was the voltage difference across the wires depending on flow velocity and the angle of sensor positioning with respect to the velocity vector. Functions $F(r_0, l, h, \phi)$, $F(r_0, l, h, \psi)$ were determined from measurement data, then compared to the theoretical results. Any deviations from the theoretical model were explained as the consequence of thermal convection and deformation of the velocity field due to the presence of wires and support prongs.

Two families of characteristic curves are considered depending on whether the hot wires rotate within the plane determined by the wires or whether they turn round the wires' axis of symmetry, that is the plane determined by the wires rotates.

Key words: thermal anemometers, hot-wire anemometers, flow reversal, flow reversal detectors.

W artykule analizuje się teoretyczne i eksperymentalne charakterystyki kątowe czujnika dwuwłóknowego z oddziaływaniem cieplnym pracującego w układzie bezmostkowego anemometru stałotemperaturowego. Przypadek, gdy płaszczyzna utworzona przez włókna jest równoległa do prędkości przepływu a same włókna pozostają do niej prostopadłe jest

* WYDZIAŁ INŻYNIERII MECHANICZNEJ I ROBOTYKI, AKADEMIA GÓRNICZO-HUTNICZA, 30-059 KRAKÓW, AL. MICKIEWICZA 30

** INSTYTUT MECHANIKI GÓROTWORU, POLSKA AKADEMIA NAUK, 30-059 KRAKÓW, UL. REYMONTA 27

opisany teoretycznie w pracy (Kiełbasa 2000 a). Tu rozpatruje się przypadek ogólny, gdzie prędkość przepływu może być dowolnie ustawiona w stosunku do czujnika. Położenie to określają dwa kąty: ϕ który jest kątem między wektorem prędkości a normalną do włókien i kąt ψ będący kątem pomiędzy wektorem prędkości a płaszczyzną, w której leżą włókna. Podano ogólne rozwiązanie na różnicę temperatur między włóknami. Przeprowadzono obliczenia numeryczne dla kilku prędkości przepływu powietrza. Wyniki ilustrują krzywe na Rys. 4–7. Krzywe teoretyczne rozróżnia odległość międzywłóknowa.

Kilka czujników poddano badaniom eksperymentalnym w tunelu aerodynamicznym. Metodykę postępowania opisano w pracy (Kiełbasa — 2000 a). Czujnik zamocowany w specjalnym obrotowym uchwycie umieszczono w tunelu aerodynamicznym. Mierzono różnicę napięć na włóknach jako funkcję prędkości przepływu i kąta ustawienia sondy w stosunku do wektora prędkości. Z danych pomiarowych wyznaczono opisane funkcje $F(r_0, I, h, \phi)$ i $F(r_0, I, h, \psi)$ porównywano z danymi wyliczonymi z teorii. Odchylenia od teoretycznego modelu wyjaśniono wpływem konwekcji cieplnej oraz deformacją pola prędkości wywołaną włóknami i wspornikami.

W eksperymencie rozpatruje się dwie rodziny charakterystyk kątowych w zależności od tego czy obrót grzanych włókien czujnika odbywa się w płaszczyźnie wyznaczonej przez te włókna czy też obrót następuje wokół osi symetrii włókien czyli obraca się płaszczyzna włókien.

Słowa kluczowe: anemometr cieplny, termoanemometr, odwrócenie przepływu, indykator zwrotu przepływu.

NOMENCLATURE

c — specific heat of the flowing medium at constant pressure,
l — distance between the hot wires,
n — overheat ratio for two wires (connected in series),
v — velocity of the flowing gas,
T_1 — temperature of the first wire,
T_2 — temperature of the second wire,
ΔT — difference in wires' temperatures,
κ — thermal diffusion coefficient of the flowing medium,
λ — thermal conductivity of the flowing medium,
ϱ — density of the flowing medium.

1. Introduction

The paper of Kiełbasa (2000 a) presents the mathematical model of a thermal detector of flow reversal, consisting of two wires connected in series (Fig. 1) and supplied from one CTA circuit (Fig. 2). The wires in the modelled sensor are of infinite length and parallel, thus determining a plane. It is also assumed that the velocity vector is perpendicular to the wire and parallel to the plane determined by them.

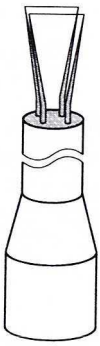

Fig. 1. Schematic diagram of the sensor

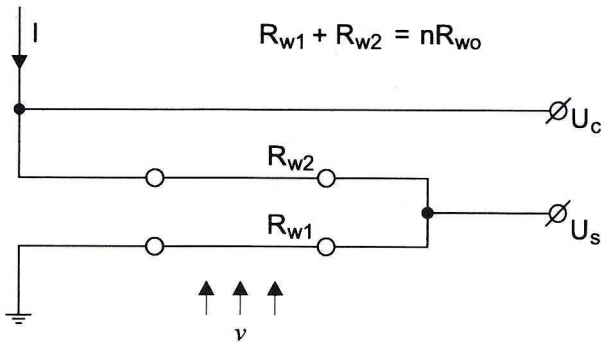

Fig. 2. Connection between the sensor wires and the supply circuit

It was explained in the quoted paper that the temperature difference ΔT between the wires in such conditions can be given by the formula:

$$\Delta T = \frac{2(n-1)}{\gamma T_g} \frac{K_0(|hr_0|)\sinh(\mathrm{hr}_0) + \mathrm{K}_0(|\mathrm{hl}|)\sinh(\mathrm{hl})}{K_0(|hr_0|)\cosh(\mathrm{hr}_0) + \mathrm{K}_0(|\mathrm{hl}|)\cosh(\mathrm{hl})}, \tag{1}$$

where:

$$h = \frac{v}{2\kappa}, \tag{2}$$

$$\kappa = \frac{\lambda}{\varrho c}, \tag{3}$$

l — distance between the wires; n — wire overheating ratio; r_0 — wire radius.

It can be easily seen that though the case considered here is relatively simple, the temperature difference is described with a very complex formula involving the Bessel

function of the zero order and hyperbolic functions. The independent variable involves the parameter h depending on velocity v which may change its sign.

In general case it need not be so. The situation is presented in Fig. 3.

The coordinate system is related to the measuring sensor in the following manner:

1. x-axis is perpendicular to the sensor wires,
2. z-axis is parallel to the sensor wires,
3. y-axis is normal to the plane $x-y$,
4. the origin of the coordinate system is on the wires' axis of symmetry,
5. the coordinate system is right-handed.

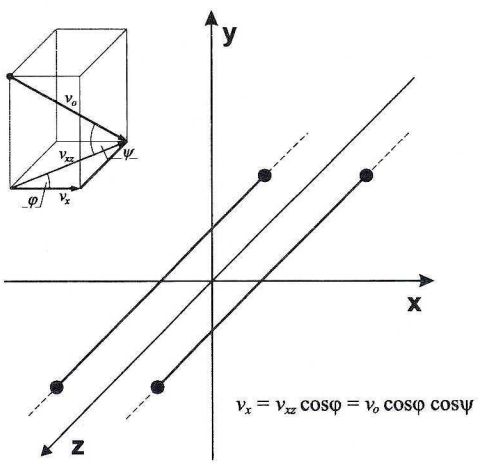

Fig. 3. Position of the two-wire sensor with respect to the flow

In thus chosen coordinate system the velocity vector can be resolved into the components, v_z, v_y, v_z, which can be given as follows:

$$v_x = v_0 \cos\phi \cos\psi\,, \tag{4}$$

$$v_y = v_0 \sin\phi, \tag{5}$$

$$v_z = v_0 \sin\psi \cos\psi\,. \tag{6}$$

The temperature distribution in the plane $x-y$ is determined only by the velocity component v_x. The v_z component is of no consequence here as we assume that the hot wires are so long that edge effects can be neglected and the velocity profile remains constant.

We can consider specific cases of characteristics depending on the angles ϕ and ψ. When $\psi = 0$ and $\phi = 0$ or π we get a flow reversal detector whose theoretical characteristics are given in the work of Kiełbasa (2000 a).

When $\psi = 0$ and ϕ is variant (i.e. the sensor revolves round the y-axis only) we get the characteristics called the characteristics of the first type. When $\phi = 0$ and ψ is variant (the sensor revolves round the z-axis) we get the characteristics of the second type.

2. Characteristics of the first type

In order to determine the angle-dependent characteristics of the first type ($\psi = 0$) we have to replace the relationship (2) present in (1) with the following expression:

$$h(\phi) = \frac{v_0}{2\kappa}\cos(\phi). \tag{7}$$

We have to bear in mind that the plane determined by the wires remains parallel to the velocity vector whereas ϕ is the angle between the velocity vector and the normal to the wires.

3. Characteristics of the second type

The angle-dependent characteristics of the second type ($\phi = 0$) will be obtained when we substitute the following expression into (1):

$$h(\psi) = \frac{v_0}{2\kappa}\cos(\psi). \tag{8}$$

In this case the velocity vector is perpendicular to the wires whereas is the angle between the velocity vector and the plane determined by the wires.

4. General case of two-wire sensor positioning in the flowing stream

In the general case of sensor positioning both angles ϕ and ψ are different from zero. According, the velocity component v_x on the plane determined by the wires (see Fig. 3) will be given as:

$$v_x = v_0 \cos\psi \cos\phi. \tag{9}$$

The temperature difference $\Delta T(\phi, \psi)$ will be given as:

$$\Delta T(\psi, \phi) =$$

$$= \frac{2(n-1)}{\gamma} \frac{K_0(|h(\psi, \phi) r_0|)\sinh(h(\psi, \phi) r_0) + K_0(|h(\psi, \phi) l|)\sinh(h(\psi, \phi) l)}{K_0(|h(\psi, \phi) r_0|)\cosh(h(\psi, \phi) r_0) + K_0(|h(\psi, \phi) l|)\cosh(h(\psi, \phi) l)} = \tag{16}$$

$$= \frac{2(n-1)}{\gamma} F(r_0, l, h(\psi, \phi)),$$

where

$$F(r_0, l, h(\psi, \phi)) = \frac{K_0(|h(\psi, \phi) r_0|) \sinh(h(\psi, \phi) r_0) + K_0(|h(\psi, \phi) l|) \sinh(h(\psi, \phi) l)}{K_0(|h(\psi, \phi) r_0|) \cosh(h(\psi, \phi) r_0) + K_0(|h(\psi, \phi) l|) \cosh(h(\psi, \phi) l)} \quad (11)$$

and

$$h(\psi, \phi) = \frac{v_0}{2\kappa} \cos\psi \cos\phi . \quad (12)$$

5. Calculations of angle-dependent characteristics — theoretical examples

The function $F(r_0, l, h, \phi, \psi)$ is strongly nonlinear and its shape pattern depends on the mutual relation between l and r_0. Let us introduce two dimensionless parameters:

$$\xi = \frac{v r_0}{2\kappa} \quad \text{and} \quad \zeta = \frac{v l}{2\kappa}.$$

Accordingly, the function $F(...)$ will be expressed as:

$$F(\xi, \zeta, \psi, \phi) = \frac{K_0(|\xi, \psi, \phi|) \sinh(\xi, \psi, \phi) + K_0(|\zeta, \psi, \phi|) \sinh(\zeta, \psi, \phi)}{K_0(|\xi, \psi, \phi|) \cosh(\xi, \psi, \phi) + K_0(|\zeta, \psi, \phi) l|) \cosh(\mathrm{h}(\psi, \phi)}. \quad (13)$$

Theoretical characteristics of two-wire anemometric sensor were then analysed numerically, on the basis of the following assumptions:

1. the flowing medium is air ($\kappa = 0.18$ cm^2/s),
2. hot wire diameter is 10 μm, accordingly $r_0 = 5.0$ μm,
3. flow velocity ranges from 0 to 0.3 m/s,
4. sensor length is 10 mm (this parameter does not appear here as it is assumed that the hot wires are of infinite length),
5. distance between the wires equals 100 or 200 times the wire radius.

Accordingly, the variability range of function arguments present in those expressions is as follows:

$$0 < \frac{v r_0}{2\kappa} = \xi \leqslant 0.42$$

and

$$0 < \frac{v l}{2\kappa} = \zeta \leqslant 100\,\xi \quad \text{or} \quad 200\,\xi.$$

In further calculations $\xi = \frac{vr_0}{2\kappa}$ was taken from the range 0.007 to 0.042, with the step 0.007. That corresponded to the change in air flow velocity every 5 cm/s. ζ ranged from 0.7 to 4.2 or from 1.4 to 8.4 (which corresponded to 100 ξ or 200 ξ) throughout the whole range of variability of ϕ or ψ, or with the step 5°.

5.1. Characteristics of the first type

The angle ϕ varied from 0 to 355°, with the step 5°. The results are presented in Fig. 4, 5, 6, 7. For the sake of clarity those results are presented in the Cartesian system and radar-shaped polar system.

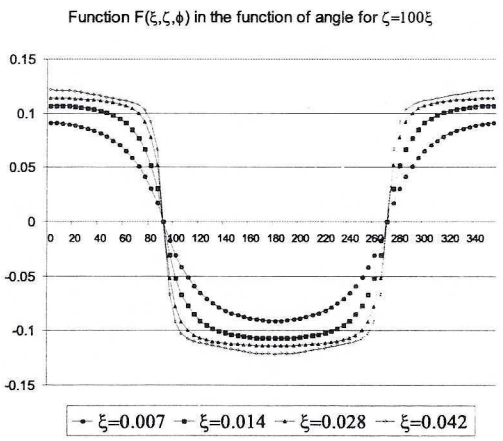

Fig. 4. Function $F(\xi, \zeta, \phi)$ in the function of angle ϕ

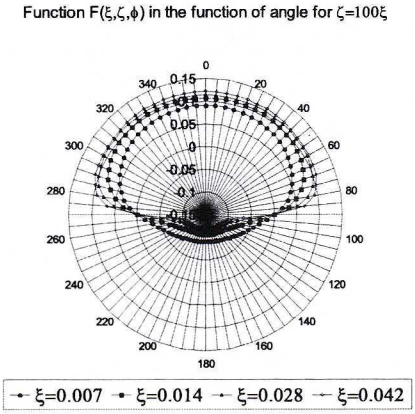

Fig. 5. Function $F(\xi, \zeta, \phi)$ in the function of angle ϕ, (radar-shaped diagram)

5.2. Characteristics of the second type

Theoretical characteristics of the second type are analogous to those of the first type. The only change is that instead of ϕ we have ψ.

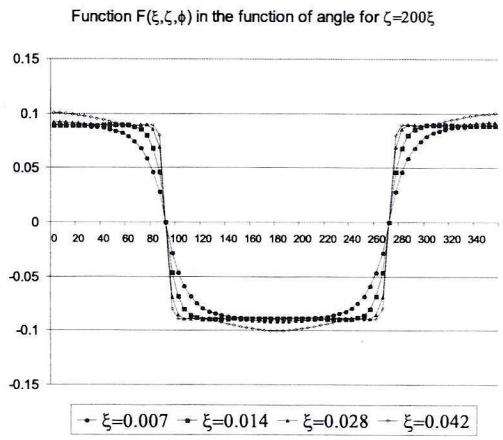

Fig. 6. Function $F(\xi, \zeta, \phi)$ in the function of angle ϕ

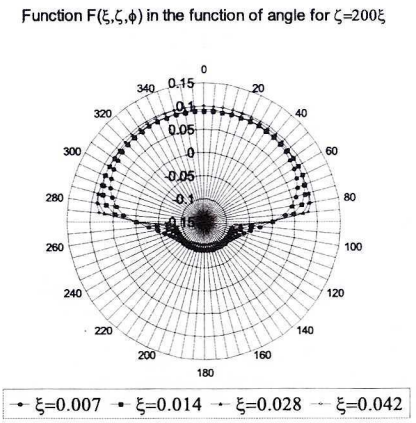

Fig. 7. Function $F(\xi, \zeta, \phi)$ in the function of angle ϕ, (radar-shaped diagram)

6. Theoretical characteristics — conclusions

The results of numerical computations lead us to the following conclusions:

1. In the case of directional characteristics of the first type the sensor displays the highest sensitivity $\left(\text{the greatest absolute value of } \frac{\partial F}{\partial \phi}\right)$ for $\phi = 0^{\circ}$ or 180°. That agrees

well with our intuition as in this case the velocity vector is parallel to the wire (it does not lie on the plane determined by the wires).

2. When directional characteristics of the second type are considered, the highest sensitivity $\left(\text{the greatest absolute value of } \frac{\partial F}{\partial \psi}\right)$ of the sensor is found for $\psi = 0$ or 180°. That also agrees well with our intuition as the velocity vector is normal to the wire.

3. On the characteristics of the first type the maximal value (the modulus) of the function $F(r_0, l, h, \phi)$ is found for 90° and 270°. These maximal points are not clearly marked. This is a very favourable feature of two-wire sensor as the flow reversal detector since its "angle of viev" is thus expanded.

4. On the characteristics of the second type the maximal value [the modulus] of the function $F(r_0, l, h, \psi)$ is found for 90° and 270°. These maximal points are not clearly marked, either. This is a very favourable feature of two-wire sensor as the flow reversal detector since its "angle of view" is thus expanded.

5. "Flattened" characteristics presented in Fig. 6 are another interesting feature. They are the result of specific interactions between functions $K_0(...)\sinh(...)$ and $K_0(...)\cosh(...)$ of two different arguments. That particular feature stabilises the angle sensitivity of the flow reversal detector.

7. Experimental investigation of angle-dependent characteristics

Angle-dependent characteristics of two-wire sensors supplied from CTA were investigated using the facilities described in the work of Kiełbasa (2000 a). To obtain the characteristics of the first type (Fig. 8, 9, 10 & 11), the wires were arranged vertically and the plane they determined was parallel to the velocity vector. The sensor holder, whose axis is normal to the wires, is fitted in a rotating arm (rotor) driven by a step motor. The whole assembly (sensor + rotor + motor) is put in the wind tunnel in such a manner that the sensor coincides with the tunnel axis. When characteristics of the second type (Fig. 12, 14, 14 & 15) were investigated, the sensor was fixed in a special holder providing the position control so that at first the two wires would determine a horizontal plane.

TABLE

Parameters of tested sensors

No.	Wire material	Wires diameter μm	Distance between wires mm	Wire overheating	Type of characteristic
1	Tungsten	10	0.5	1.4	I
2	Tungsten	8	1.82	1.8	I
3	Tungsten	10.5	0.5	1.8	II
4	Tungsten	8	0.68	1.8	II

When this plane rotated, the hot wires were still normal to the velocity vector. These two situations are presented in both in Fig. 16 and 17.

Sensors whose parameters are summarised in Table were investigated. Functions $F(r_0, l, v, \phi)$ or $F(r_0, l, v, \psi)$ were obtained experimentally, on the basis of measured voltages across the wires $-U_c$ and U_s (see Fig. 2), in accordance with the formula introduced by Kiełbasa (2000 b):

$$F(r_0, l, v, \phi) = \frac{\gamma}{2(n-1)} \Delta T = \frac{n}{2(n-1)} \frac{2U_s - U_c}{U_c}, \tag{4}$$

where γ is the coefficient of wire thermal resistance.

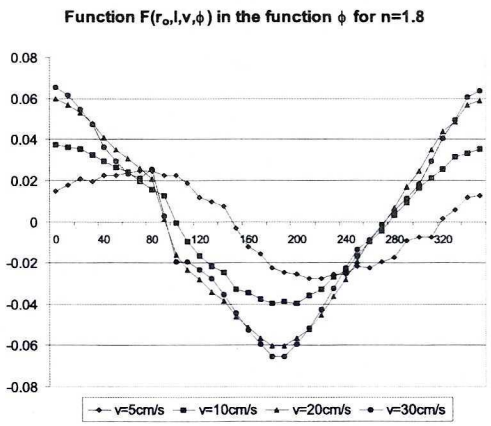

Fig. 8. Function $F(r_0, l, v, \phi)$ in the function of ϕ for $r_0 = 5$ μm, $l = 0.5$ mm; $n = 1.8$. (Cartesian coordinates, characteristics of the first type)

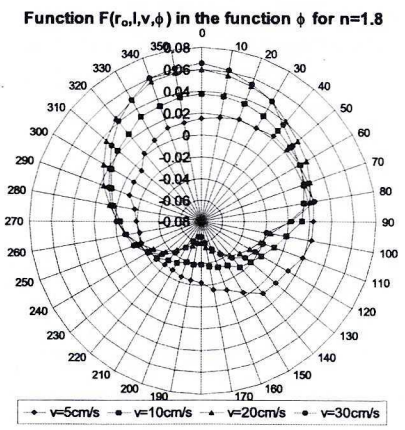

Fig. 9. Function $F(r_0, l, v, \phi)$ in the function of ϕ for $r_0 = 5$ μm, $l = 0.5$ mm; $n = 1.8$ (radar-shaped diagram, characteristics of the first type)

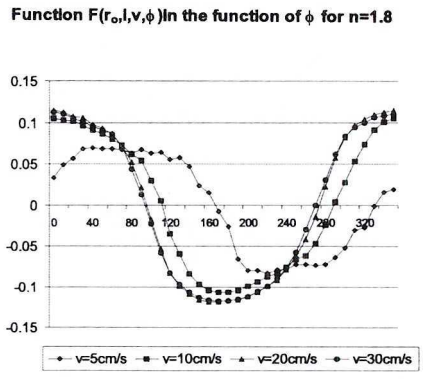

Fig. 10. Function $F(r_0, l, v, \phi)$ in the function of ϕ for $r_0 = 5$ μm, $l = 1.82$ mm; $n = 1.8$. (Cartesian coordinates, characteristics of the first type)

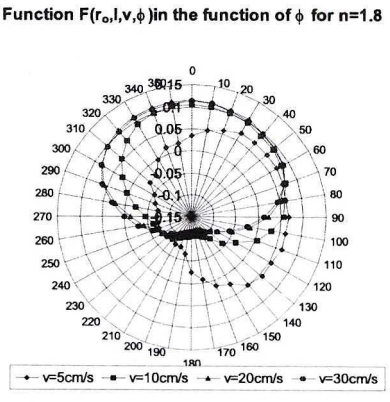

Fig. 11. Function $F(r_0, l, v, \phi)$ in the function of ϕ for $r_0 = 5$ μm, $l = 1.82$ mm; $n = 1.8$. (radar-shaped diagram; characteristics of the first type)

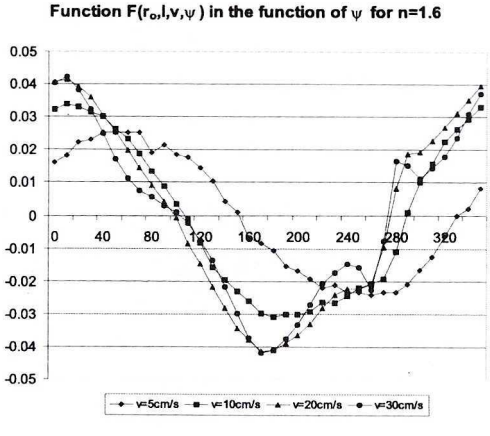

Fig. 12. Function $F(r_0, l, v, \phi)$ in the function of ψ for $r_0 = 5$ μm, $l = 0.5$ mm; $n = 1.6$. (Cartesian coordinates, characteristics of the second type)

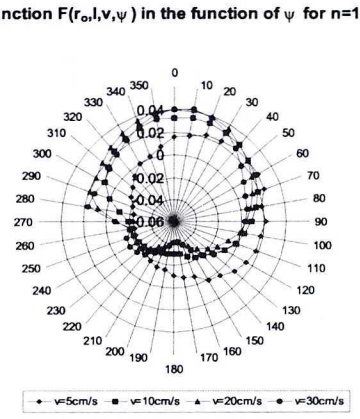

Fig. 13. Function $F(r_0, l, v, \phi)$ in the function of ψ for $r_0 = 5$ μm, $l = 0.5$ mm; $n = 1.6$ (radar-shaped diagram, characteristics of the second type)

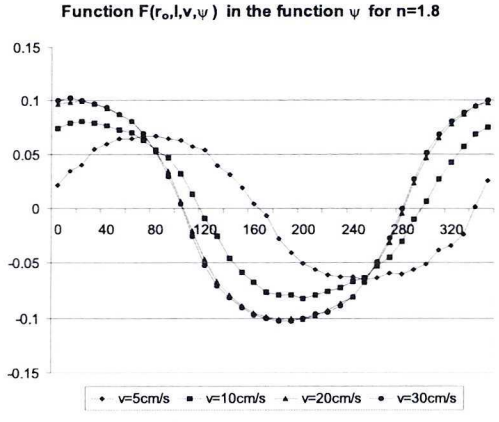

Fig. 14. Function $F(r_0, l, v, \phi)$ in the function of ψ for $r_0 = 4$ μm, $l = 0.68$ mm; $n = 1.8$. (Cartesian coordinates)

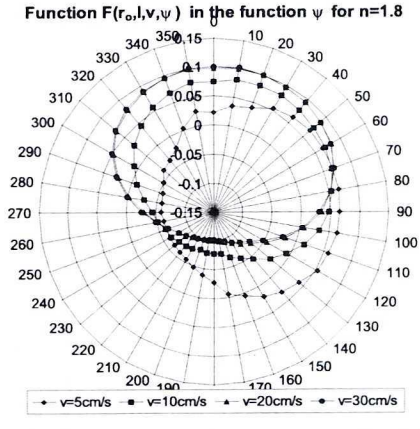

Fig. 15. Function $F(r_0, l, v, \phi)$ in the function of ψ for $r_0 = 4$ μm, $l = 0.68$ mm; $n = 1.8$ (radar-shaped diagram, characteristics of the second type)

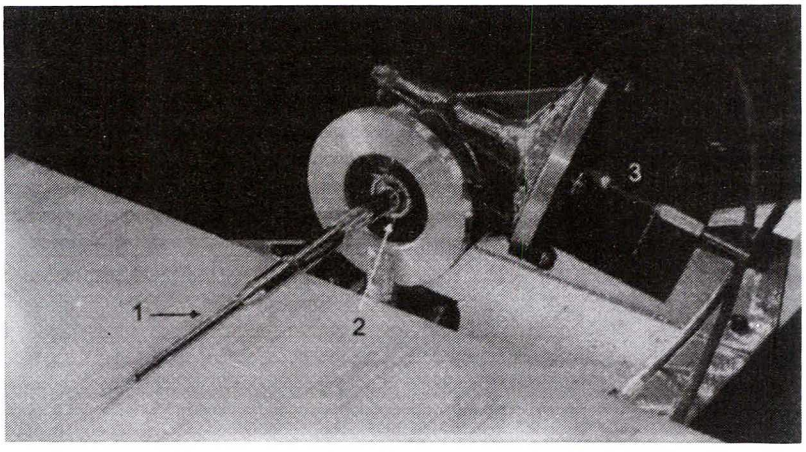

Fig. 16. A holder turning the sensor in the plane determined by the wires (angle-dependent characteristics of the first type). *1* — sensor fixed in a rotating holder, *2* — rotor, *3* — step motor driving the rotor

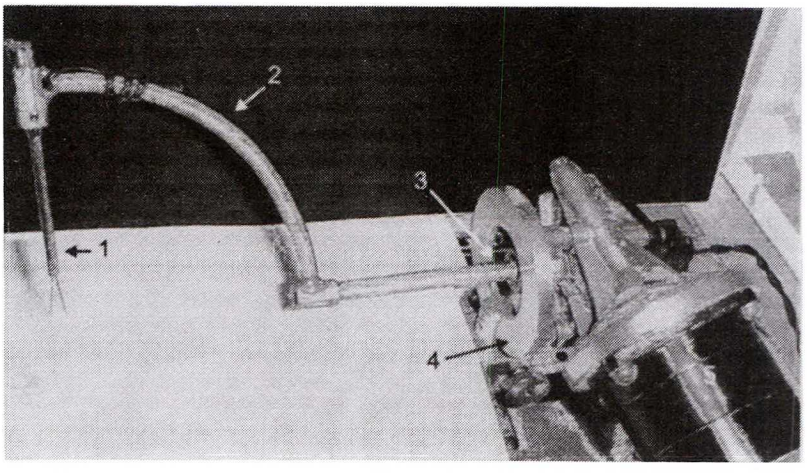

Fig. 17. A holding arm turning the sensor round the wires axis of symmetry (angle-dependent characteristics of the second type). *1* — sensor fixed in a holder; *2* — rotating arm; *3* — rotor, *4* — rotor-fitting ring; *5* — step motor

Certain inaccuracies in sensor manufacture may bring about asymmetry of wires' resistance and hence the voltages (U_s) and $(2\,U_s - U_c)$. Therefore, a symmetry factor k was introduced. The reasoning here was as follows: the sum of voltage difference ΔU_i (defined above) after N measurements should be zero. That means that the field on the side of positive values ΔU_i should be equal to that on the side of its negative values. Accordingly:

$$\sum_{i=1}^{N} \Delta U_i = \sum_{i=1}^{N} \left[(U_{c_i} - kU_{s_i}) - kU_{s_i} \right] = \sum_{i=1}^{N} (U_{c_i} - 2\,kU_{s_i}) = 0$$

hence

$$\sum_{i=1}^{N} U_{c_i} = 2k \sum_{i=1}^{N} U_{s_i}$$

and

$$k = \frac{\sum_{i=1}^{N} U_{c_i}}{2 \sum_{i=1}^{N} U_{s_i}},$$

where N stands for the number of measurements, in this case it will be 36. This parameter is taken into account in the graphs below.

8. Experimental investigation — conclusion

In qualitative terms the angle-dependent characteristics of the first and second type agree well with those obtained theoretically. Their distinctive features can be listed as follows:

1. The "angle of view" of the two-wire sensor — defined as the angle extending from the point where the voltage difference exceeded zero to the point where it became zero again — is almost 180° no matter what the type of characteristics and the overheating ratio.

2. The higher the overheating ratio and flow velocity, the higher the maximal voltage difference.

3. The angle-dependent characteristics seem to be "rounded" as the result of finite length of sensor wires. The longer the wires, the better angle sensitivity and resolution of the sensor. A certain difficulty presents itself here (which could be observed during the tests), namely for most values of overheating the wire length will increase as the result of thermal expansion, which cannot be compensated by support prongs stretching. The wires cease to be parallel, instead they start to hang loosely. In such situation the sensor characteristics will be changed, too.

4. Values of functions $F(r_0, l, v, \phi)$ and $F(r_0, l, v, \psi)$ determined experimentally are similar to theoretical ones. Minor discrepancies found for small velocities are the consequence of natural convection, which was not taken into account in the theoretical model.

5. The effect of convection are well marked at very small velocities (less than 20 cm/s). Flow velocity as "sensed" by the sensor is nearly vertical, no matter what the type of characteristics. That can be seen in all the experimental graphs and for all values of over-heating.

All things considered, it seems a two-wire sensor operating in CTA circuit can be well used for flow reversal detection. When the required technical conditions for

operation in mines are fully most (such as spark protection requirements), the sensor may be used in mines as flow reversal detector in mine workings.

*

This study is a part of the research project no 8T10C00613: "Optimisation of the thermal anemometer used as flow reversal detector" supported by the State Committee for Scientific Research, also as the part of the research programme in the field of "Flow metrology" run in accordance with statutory requirements in the Strata Mechanics Research Institute of the Polish Academy of Sciences. First results were presented during the conference "Optical and optical-electronic sensors" COE'2000 (Kiełbasa 2000 b); Gliwice — May 2000).

REFERENCES

Kiełbasa J., Ligęza P., Gawor M., 1999. Optymalizacja anemometru z oddziaływaniem cieplnym jako wskaźnika zwrotu przepływu gazu. Sprawozdanie z realizacji projektu badawczego nr 8T10C00613.

Kiełbasa J., 2000 a. Thermal sensor of flow reversal. Archives of Mining Sciences **45**, 1, pp. 89–100.

Kiełbasa J., 2000 b. Experimental verification of the theoretical model of the thermal detector of flow reversal. Archives of Mining Sciences (w druku).

Kiełbasa J., 2000 c. Dwuwłóknowy czujnik termoanemometryczny jako cieplny indykator odwrócenia przepływu. Materiały VI Konferencji „Czujniki optyczne i optoelektryczne COE'2000", Gliwice — czerwiec 2000.

Kiełbasa J., 2000 d. Kątowe charakterystyki cieplnego indykatora zwrotu przepływu. Materiały VI Konferencji „Czujniki optyczne i optoelektroniczne COE'2000", Gliwice — czerwiec 2000.

REVIEW BY: PROF. DR HAB. INŻ STANISŁAW DROBNIAK, CZĘSTOCHOWA

Received: 26 May 2000.